polymer was accomplished by placing a concentrated solution of the nanoparticles in dimethylsulfoxide onto the PLL film for about 20 min, after which it was rinsed in dimethylsulfoxide and then dichloromethane. From the molecular weight, the average length of the PLL is about 30 nm. Therefore, each polymer can accommodate about seven or eight nanoparticles.
[20] L. Clarke, M. N. Wybourne, M. Yan, S. X. Cai, J. F. W. Keana, *Appl. Phys. Lett.* **1997**, *71*, 617.
[21] A. A. Middleton, N. S. Wingreen, *Phys. Rev. Lett.* **1993**, *71*, 3198.
[22] G. Y. Hu, R. F. O'Connell, *Phys. Rev. B* **1994**, *49*, 16 773.
[23] A. J. Rimberg, T. R. Ho, J. Clarke, *Phys. Rev. Lett.* **1995**, *74*, 4714.
[24] L. Clarke, M. N. Wybourne, M. Yan, S. X. Cai, L. O. Brown, J. Hutchison, J. F. W. Keana, *J. Vac. Sci. Technol. B* **1997**, *15*, 2925.
[25] The capacitance matrix was calculated for different chain lengths using the software package FastCap MIT (**1992**). We used the nanoparticle dimensions given in the text and a ligand shell dielectric constant of 3. For nanoclusters away from the end of the chains we obtain $C_{dd} \approx 0.04$ aF and $C_g \approx 0.17$ aF. As expected, the value of C_g is slightly larger than the value calculated for an isolated metal sphere of radius a coated with a dielectric shell, $C_g \approx (4\pi\varepsilon\varepsilon_0 a)/(1+(a/d)(\varepsilon-1)) = 0.14$ aF, where d is the total radius of the core plus ligand shell.
[26] Simulations were carried out using both MOSES (Monte-Carlo Single-Electronics Simulator, R. H. Chen) and SIMON (Simulation of Nano Structures, C. Wasshuber).
[27] S. Chen, R. S. Ingram, M. J. Hostetler, J. J. Pietron, R. W. Murray, T. G. Schaaff, J. T. Khoury, M. M. Alvarez, R. L. Whetton, *Science* **1998**, *280*, 2098.
[28] L. Y. Gorelik, A. Isacsson, M. V. Voinova, B. Kasemo, R. I. Shekhter, M. Jonson, *Phys. Rev. Lett.* **1998**, *80*, 4526.
[29] O. D. Häberlen, S. C. Chung, M. Stener, N. Rösch, *J. Chem. Phys.* **1997**, *106*, 5189.
[30] Y. Awakuni, J. H. Calderwood, *J. Phys. D: Appl. Phys.* **1972**, *5*, 1038.
[31] G. Markovich, C. P. Collier, J. R. Heath, *Phys. Rev. Lett.* **1998**, *80*, 3807.
[32] C. P. Collier, R. J. Saykally, J. J. Shiang, S. E. Hendrichs, J. R. Heath, *Science* **1997**, *277*, 1978.
[33] N. Mott, *Metal Insulator Transitions*, Taylor and Francis, London **1990**.

Catalytic Growth of Zinc Oxide Nanowires by Vapor Transport**

By *Michael H. Huang*, *Yiying Wu*, *Henning Feick*, *Ngan Tran*, *Eicke Weber*, and *Peidong Yang**

Recent progress in the synthesis and characterization of nanowires has been driven by the need to understand the novel physical properties of one-dimensional nanoscale materials, and their potential application in constructing nanoscale electronic and optoelectronic devices.[1] Nanowires with different compositions have been explored using various methods including the vapor-phase transport process,[2–4] chemical vapor deposition,[5] arc discharge,[6] laser ablation,[7] solution,[8,9] and a template-based method.[10,11] While a large part of this work has been focused on semiconductor systems such as Si,[1] Ge,[2] GaN,[3,10] GaAs,[5,7] only a few studies on oxide systems exist in the literature. Among them, MgO nanowires have been synthesized and incorporated into high-temperature superconductors to improve the critical current densities of the superconductors.[12,13] Several other oxide nanowires, including SiO_2,[14] GeO_2,[4] and Ga_2O_3,[6] have also been reported although the insulating nature of these oxide systems could limit, if any, their applications. It is thus necessary to look into other oxide systems with interesting optical, electrical, and magnetic properties.

ZnO, a wide bandgap (3.37 eV) semiconductor with large exciton binding energy (60 meV), has been investigated as a short-wavelength light-emitting, transparent conducting and piezoelectric material. ZnO nanoclusters and thin films have also been shown to exhibit room temperature UV lasing properties.[15] Most of the ZnO nanomaterials studied are in the form of nanoparticles although needle crystals and large whiskers have been previously reported.[16] Polycrystalline ZnO nanowires have also been recently fabricated within a porous alumina template.[11] Due to the promising application of ZnO nanowires in nanoscale optoelectronic devices, it is important to be able to synthesize these nanowires in single-crystalline form and study their optical properties. Here we report the use of the vapor-phase transport process to grow ZnO nanowires via the vapor–liquid–solid (VLS) mechanism. The Zn vapor is generated using carbothermal or hydrogen reduction of ZnO. Size control of the nanowire diameters was achieved by varying the thickness of the thin film Au catalyst. It is also possible to grow thinner wires by using monodispersed Au colloids dispersed on substrates as catalysts. In addition, a ZnO nanowire network has been successfully synthesized on patterned Au catalysts. Photoluminescence (PL) characterization of the nanowires shows that these nanowires exhibit strong UV emission and size-dependent green light emission.

ZnO nanowires were grown on Au-coated silicon substrates by heating a 1:1 mixture of ZnO and graphite powder to 900–925 °C under a constant flow of argon for 5–30 min. The substrate surface appeared light or dark gray after the reaction, indicating the deposition of material. X-ray diffraction (XRD) patterns of ZnO nanowire samples were taken to examine the crystal structure of the nanowires. All samples gave similar XRD patterns indicating the nanowires' high crystallinity. Figure 1 shows a typical XRD pattern of the ZnO nanowires. The diffraction peaks can be indexed to a hexagonal structure of bulk ZnO with cell constants of a = 3.24 and c = 5.19 Å. While Au (111) and (200) peaks have been detected in some samples, no diffraction peaks from Zn have been found in any of our samples.

The morphology of the materials on the substrate was examined by scanning electron microscopy (SEM). A typical SEM image for nanowires grown on a substrate coated with

[*] Prof. P. Yang, Dr. M. H. Huang, Y. Wu, N. Tran
Department of Chemistry, University of California
Berkeley, CA 94720 (USA)
E-mail: pyang@cchem.berkeley.edu
Prof. E. Weber, Dr. H. Feick
Department of Materials Science and Engineering
Materials Science Division, Lawrence Berkeley National Laboratory
University of California
Berkeley, CA 94720 (USA)

[**] This work was supported by the Camille and Henry Dreyfus Foundation, 3M Corporation, and University of California, Berkeley. Work at the Lawrence Berkeley National Laboratory was supported by the Office of Science, Basic Energy Sciences, Division of Materials Science, of the U.S. Department of Energy under contract No. DE-AC03-76SF00098. We thank Vojislav Srdanov at University of California, Santa Barbara for help during the power-dependent emission measurement. We thank the Microfabrication Laboratories and the National Center for Electron Microscopy for the use of their facilities.

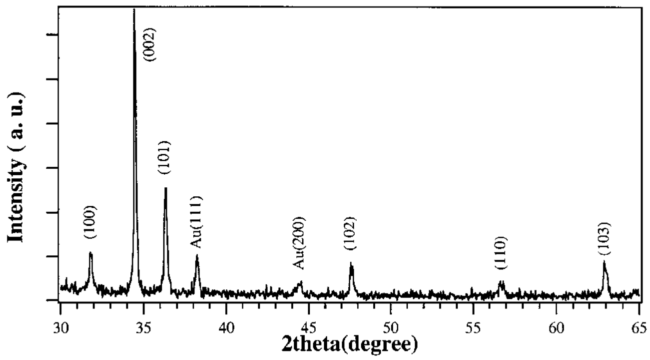

Fig. 1. XRD pattern of ZnO nanowires on a silicon (111) substrate. Indices of the peaks are specified above the peaks.

~50 Å layer of Au is shown in Figure 2a. The image shows that entangled and uniform ZnO nanowires were formed on the substrate in high yield. The diameters of the nanowires normally range from 80–120 nm and their lengths are 10–20 μm although some thinner wires (~20 nm) have also been observed. Shorter nanowires and nanoparticles were found in regions located closer to the reagent source. We found higher temperatures and longer reaction times introduced significant crystal overgrowth and produced nanowires with larger diameters.

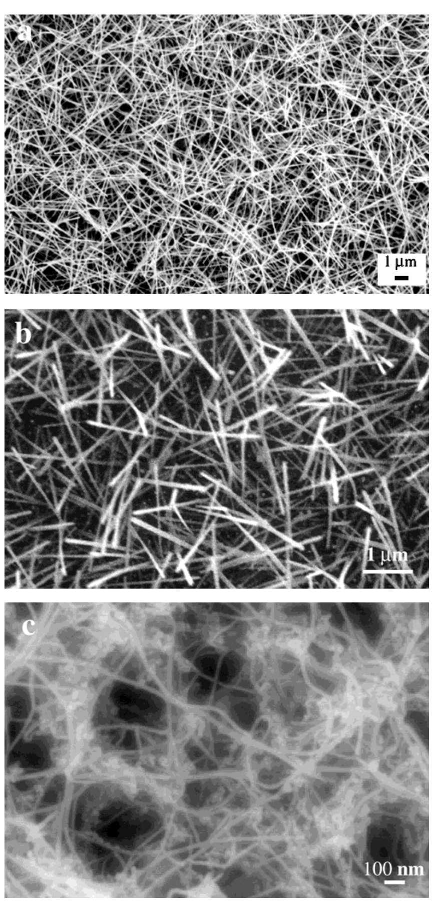

Fig. 2. a) SEM image of ZnO nanowires grown from ZnO and graphite powder in an argon flow on the surface of a silicon substrate coated with ~50 Å thick Au film. b) SEM image of ZnO nanowires grown under the same conditions as above but using a substrate coated with 30 Å thick Au film. c) SEM image of thin ZnO nanowires formed after the hydrogen thermal reduction treatment.

In an effort to grow ZnO nanowires with smaller average diameters, substrates coated with a thinner layer of Au were used. The idea is based on a possible direct correlation between the size of the catalytic particles and the resulting diameters of the nanowires. Smaller Au droplets, formed in the heating process during reaction, should favor the growth of thinner nanowires. Diameter control of silicon nanowires using Au nanoparticles in a solution-phase approach has been reported recently.[9] Silicon substrates coated with 19–30 Å Au were used to grow ZnO nanowires using the same procedure. Figure 2b shows a SEM image of ZnO nanowires grown from a substrate coated with 30 Å Au. Most of the nanowires have diameters of 40–70 nm and lengths of 5–10 μm. Nanowires with a diameter of ~100 nm, however, are still present. This observation apparently relates to the thermodynamic limit for the minimum radius of the metal–liquid clusters at high temperature

$$r_{\min} = 2\,\sigma_{LV} V_L / RT \ln s \qquad (1)$$

where σ_{LV} is the liquid–vapor surface free energy, V_L is the molar volume of liquid, and s is the vapor-phase supersaturation.[1] Nonetheless, the results showed that thinner Au layers favor the growth of thinner nanowires. In fact, Au clusters with average diameters of 25 nm and 118 nm were obtained after annealing 24 Å and 86 Å thick Au films, respectively.

A further decrease in the wire's diameter was achieved through the hydrogen reduction of the as-made ZnO nanowires. During this process, the as-made wires were treated in a hydrogen flow at 525–575 °C for 30 min. Figure 2c shows a SEM image of thin ZnO nanowires after the thermal treatment. Extensive growth of long (5–10 μm) and thin (20–30 nm) wires on the substrate was observed. However, these thin ZnO wires apparently are newly grown nanowires since they are located in different areas of the substrate. Selected area electron diffraction confirmed the single-crystalline nature of these thin ZnO nanowires. In fact, direct hydrogen reduction of ZnO powder also yields thin nanowires (20–30 nm thick, 1–5 μm long) on Au coated substrates. The exact reason why the hydrogen reduction yields thinner wires than carbothermal reduction is currently under investigation. Alternatively, Au nanoclusters (15 nm) have also been used to produce thinner nanowires. The Au nanoclusters were dispersed on silicon substrates or within mesoporous silica SBA-15 films[17] to minimize possible aggregation. Nanowires with diameters of 20–50 nm were observed after the growth.

Additional structural characterization of the ZnO nanowires was carried out using transmission electron microscopy (TEM). Figure 3a shows a TEM image of a thin nanowire with an alloy tip. The presence of the alloy tip is indicative of a growth process by the VLS mechanism. Such tips have been found for nanowires grown by both the graphite and hydrogen reduction methods. Figure 3b shows a high-resolution TEM image of a single-crystalline ZnO nanowire. The spacing of 2.56 ± 0.05 Å between adjacent lattice planes corresponds to

  0935-9648/01/0201-0114 $ 17.50+.50/0

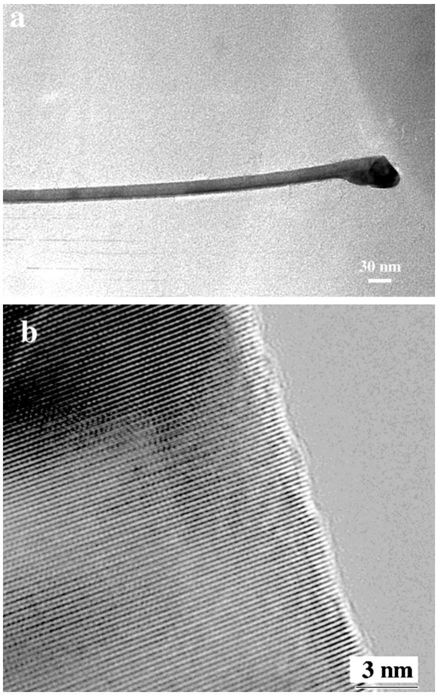

Fig. 3. a) TEM image of a thin ZnO nanowire with a Zn/Au alloy tip. b) High-resolution TEM image of a single-crystalline ZnO nanowire showing the lattice fringes.

the distance between two (002) crystal planes, indicating <001> as the growth direction for the ZnO nanowires. This <001> preferential growth direction is also reflected in the high diffraction intensity of (001) peaks in Figure 1.

Although the VLS crystal growth mechanism has been widely used for semiconductor nanowire growth,[1–9] oxide nanowire growth through the VLS mechanism could be complicated by the presence of the oxygen since most oxides have very high melting points. In this study, the process involves the reduction of ZnO powder by graphite/hydrogen to form Zn and CO/H_2O vapor at a high temperature. The Zn vapor is transported to, and reacted with, the Au catalyst on silicon substrates located downstream at a lower temperature to form alloy droplets. As the droplets become supersaturated, crystalline ZnO nanowires are formed, possibly by the reaction between Zn and CO/H_2O at a low temperature. The presence of a small amount of CO/H_2O is not expected to significantly change the Au–Zn phase diagram, at the same time they act as the oxygen source during the ZnO nanowire growth. In fact, control experiments without graphite in the starting materials essentially produced nothing on the Au coated substrates, which also indicates the importance of the Zn vapor generated by the carbothermal reduction of ZnO. We also note that the size of the nanowires generally is larger than the starting Au catalyst sizes by 5–15 nm due to the initial Au–Zn alloying process.

ZnO nanowire growth through the VLS mechanism also allows us to pattern these wires into a network. Initial patterning experiments used a 300 mesh copper grid with a hexagonal pattern as a mask during the Au deposition. Nanowire growth was then carried out by the carbothermal reduction of ZnO in an Ar flow. SEM studies (Fig. 4a) reveal extensive growth of fine, long, and flexible ZnO nanowires from the edges of the hexagons. The wire growth conforms to the hexagonal pattern of the copper grid in high fidelity. Most of the wires actually bridge the neighboring metal hexagons and form an intricate network. Figure 4b shows a SEM image of the same sample at a higher magnification to reveal more detail. The nanowires at the edge have a diameter of about 50–200 nm, and can be over 50 μm long. In the hexagon center, larger features were observed presumably due to the different gold film thickness at the hexagon edge and center as a result of the shadow mask deposition. This controlled growth of nanowires to form certain patterns and the eventual control of wire growth at certain locations may have implications for potential applications in nanoscale devices.

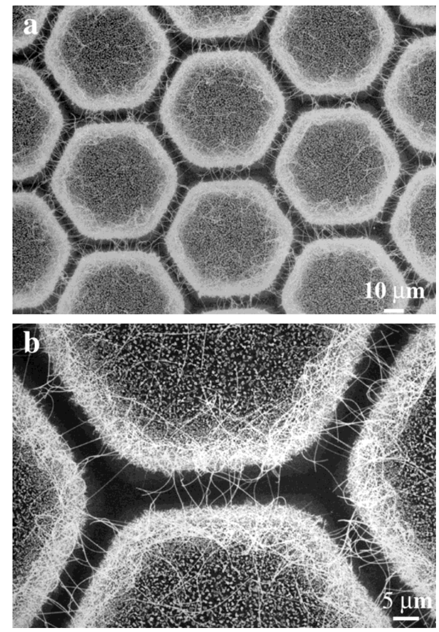

Fig. 4. a) SEM image of ZnO nanowire networks grown from the patterned Au islands. b) SEM image of the same sample at a higher magnification.

Photoluminescence (PL) spectra of nanowires of different diameters were measured using a He–Cd laser (325 nm) as the excitation source. Figure 5 shows the room temperature PL spectra of nanowires with an average diameter of 100, 50, and 25 nm. Strong emission at ~380 nm was observed for all nanowires. In addition, we observed increasing green light emission intensity at ~520 nm (506 nm for 25 nm wires) when decreasing the nanowire sizes. Whilst the UV emission corresponds to the near band-edge emission, the green emission peak is commonly referred to as a deep-level or trap-state emission. The green transition has been attributed to the singly ionized oxygen vacancy in ZnO and the emission results from the radiative recombination of a photogenerated hole with an electron occupying the oxygen vacancy.[18] The progressive increase of the green light emission intensity relative to the UV emission as the wire diam-

  0935-9648/01/0201-0115 $ 17.50+.50/0

ADVANCED MATERIALS

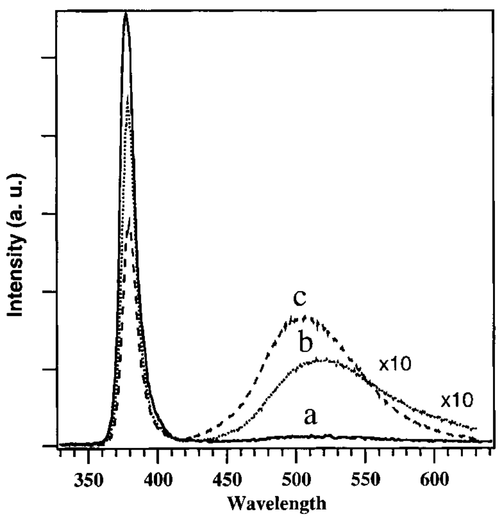

Fig. 5. Photoluminescence spectra of ZnO nanowires of different diameters recorded at room temperature. Spectra a, b, and c correspond to nanowires with average diameters of 100, 50, and 25 nm, respectively.

eter decreases suggests that there is a greater fraction of oxygen vacancies in the thinner nanowires. We believe higher surface area to volume ratio for thinner wires should favor a higher level of surface and sub-surface oxygen vacancies under the current reductive environment. Furthermore, preliminary power-dependent PL measurements were performed to investigate the possibility of amplified spontaneous emission (ASE) from 50 nm thick wires. 355 nm radiation from a Q-switched Nd–YAG laser operating at 10 Hz was used as the excitation source. A slight red shift of the near band-edge emission, as well as an increase in peak intensity, were observed upon increasing the laser power. Such a phenomenon has been observed before in microcrystalline thin ZnO films and may indicate the presence of stimulated emission.[19] Further work is underway to demonstrate possible ASE or lasing from these nanowires.

In summary, we have described the synthesis of highly crystalline ZnO nanowires via a VLS growth mechanism using Au as catalyst. Diameter control of the nanowires was achieved by varying the Au layer thickness and by using the hydrogen reduction method. Patterned nanowire network growth has also been demonstrated. Room-temperature photoluminescence spectra of the nanowires show the near band-edge emission and the deep-level green light emission. An enhanced deep-level emission for thinner nanowires has been observed and attributed to their larger surface area. We believe these nanowires could be used as light-emitting devices in nanoscale optoelectronic applications.

Experimental

Silicon substrates were cleaned in a sonicating bath of acetone for about 1 h. The substrates were coated with a layer of Au using a Denton Vacuum Desk II cold sputter unit (~50 Å) or a Veeco 401 vacuum thermal evaporator with a quartz crystal thickness monitor for exact Au film thickness (19–100 Å). An equal amount of ZnO powder (Alfa Aesar, 99.999 %) and graphite powder (Alfa Aesar, 99 %) were ground and transferred to an alumina boat. The Au-coated Si substrates and the alumina boat were placed in a small quartz tube. The substrates were typically placed 0.5–10 cm from the center of the boat. This quartz tube was then placed inside a furnace quartz tube, with the center of the alumina boat positioned at the center of the furnace and the substrates placed downstream of an argon flow. The temperature of the furnace was ramped to 890 or 925 °C at a rate of 50–100 °C/min and typically kept at that temperature for 1–30 min under a constant flow of argon (20–25 standard cubic cm). After the furnace had cooled to room temperature, light or dark gray material was found on the surface of the substrates. For the patterned growth of ZnO nanowires, a 300 mesh (~30 µm regular hexagonal opening) copper grid was used as a mask during the Au deposition (50–100 Å thick). For growing ZnO nanowires using Au nanoclusters, uniform Au colloids (average 15 nm) were dispersed on the surface of SiO_2 coated Si substrates or embedded in mesoporous SBA-15 thin films by spin coating [17].

The crystal structure of the nanowires was analyzed using XRD (Siemens D5000). The morphology and size distribution of the nanowires were characterized using SEM (JEOL6400 or JSM-6430 operated at 5 KeV) and verified by TEM (Topcon 002B and JEOL 200 CX operated at 200 keV). High-resolution TEM images of the wires were recorded with a Philips CM200 operated at 200 keV.

For the photoluminescence studies, a chopped He–Cd laser (325 nm, Omnichrom 3074-30M) with an output power of 10 mW was used as the excitation source for the emission spectra. The luminescence light was dispersed by a double grating spectrometer (0.85 m, 1800 grooves/mm, SPEX 1404) and detected by a standard GaAs photomultiplier tube using a conventional lock-in technique (lock-in amplifier, Stanford Research Systems SR530).

Received: July 10, 2000
Final version: October 2, 2000

[1] J. T. Hu, T. W. Odom, C. M. Lieber, *Acc. Chem. Res.* **1999**, *32*, 435.
[2] Y. Wu, P. Yang, *Chem. Mater.* **2000**, *12*, 605.
[3] C. C. Chen, C. C. Yeh, *Adv. Mater.* **2000**, *12*, 738.
[4] Z. G. Bai, D. P. Yu, H. Z. Zhang, Y. Ding, X. Z. Gai, Q. L. Hang, G. C. Xiong, S. Q. Feng, *Chem. Phys. Lett.* **1999**, *303*, 311.
[5] M. Yazawa, M. Koguchi, A. Muto, M. Ozawa, K. Hiruma, *Appl. Phys. Lett.* **1992**, *61*, 2051.
[6] Y. C. Choi, W. S. Kim, Y. S. Park, S. M. Lee, D. J. Bae, Y. H. Lee, G.-S. Park, W. B. Choi, N. S. Lee, J. M. Kim, *Adv. Mater.* **2000**, *12*, 746.
[7] a) X. F. Duan, C. M. Lieber, *Adv. Mater.* **2000**, *279*, 208. b) A. M. Morales, C. M. Lieber, *Science* **1998**, *279*, 208.
[8] T. J. Trentler, K. M. Hickman, S. C. Goel, A. M. Viano, P. C. Gibbons, W. E. Buhro, *Science* **1995**, *270*, 1791.
[9] J. D. Holmes, K. P. Johnston, R. C. Doty, B. A. Korgel, *Science* **2000**, *287*, 1471.
[10] a) M. H. Huang, A. Choudrey, P. Yang, *Chem. Commun.* **2000**, *12*, 1603. b) J. Zhu, S. Fan, *J. Mater. Res.* **1999**, *14*, 1175.
[11] Y. Li, G. W. Meng, L. D. Zhang, F. Phillipp, *Appl. Phys. Lett.* **2000**, *76*, 2011.
[12] P. Yang, C. M. Lieber, *Science* **1996**, *273*, 1836.
[13] P. Yang, C. M. Lieber, *US Patent 5 897 945*.
[14] Y. Q. Zhu, W. B. Hu, W. K. Hsu, M. Terrones, N. Grobert, J. P. Hare, H. W. Kroto, D. R. M. Walton, H. Terrones, *J. Mater. Chem.* **1999**, *9*, 3173.
[15] a) H. Cao, J. Y. Xu, D. Z. Zhang, S.-H. Chang, S. T. Ho, E. W. Seelig, X. Liu, R. P. H. Chang, *Phys. Rev. Lett.* **2000**, *84*, 5584. b) H. Cao, J. Y. Xu, E. W. Seelig, R. P. H. Chang, *Appl. Phys. Lett.* **2000**, *76*, 2997. c) D. M. Bagnall, Y. F. Chen, Z. Zhu, T. Yao, S. Koyama, M. Y. Shen, T. Goto, *Appl. Phys. Lett.* **1997**, *70*, 2230.
[16] a) T. Matsushita, K. Kodaira, J. Saito, R. Shida, *J. Cryst. Growth* **1974**, *26*, 147. b) S. D. Sharma, S. C. Kashyap, *J. Appl. Phys.* **1971**, *42*, 5302. c) H. Iwanaga, N. Shibata, O. Nittono, M. Kasuga, *J. Cryst. Growth* **1978**, *45*, 228.
[17] P. Yang, T. Deng, D. Zhao, P. Feng, D. Pine, B. F. Chmelka, G. M. Whitesides, G. D. Stucky, *Science* **1998**, *282*, 2244.
[18] K. Vanheusden, W. L. Warren, C. H. Seager, D. R. Tallant, J. A. Voigt, B. E. Gnade, *J. Appl. Phys.* **1996**, *79*, 7983.
[19] a) P. Zu, Z. K. Tang, G. K. L. Wong, M. Kawasaki, A. Ohtomo, H. Koinuma, Y. Segawa, *Solid State Commun.* **1997**, *103*, 459. b) D. M. Bagnall, Y. F. Chen, M. Y. Shen, Z. Zhu, T. Goto, T. Yao, *J. Cryst. Growth* **1998**, *184/185*, 605.

  0935-9648/01/0201-0116 $ 17.50+.50/0